Production of polyhydroxyalkanoate nanoparticles using a green solvent

Received: 13 October 2021 | Revised: 28 January 2022 | Accepted: 15 February 2022

DOI: 10.1002/app.52319

ARTICLE

Applied Polymer SCIENCE WILEY

Production of polyhydroxyalkanoate nanoparticles using a green solvent

Jianhua Zhang | **Marlene J. Cran**

Institute for Sustainable Industries and Liveable Cities, Victoria University, Melbourne, Australia

Correspondence
Marlene Cran, Institute for Sustainable Industries and Liveable Cities, Victoria University, PO Box 14428, Melbourne, VIC 8001, Australia.
Email: marlene.cran@vu.edu.au

Abstract

Biopolymer nanoparticles (NPs) produced from poly(3-hydroxybutyrate-co-3-hydroxyvalerate) (PHBV) are typically formed by first dissolving the polymer in organic solvents. In order to eliminate the use of toxic solvents, an alternative "green" solvent system using glacial acetic acid was used in this study for the preparation of NPs via nanoprecipitation. The influence of various factors on the resulting particle size was investigated including the use of an emulsifying agent, temperatures of stock and receiving solutions, and concentration of stock solution. The addition of emulsifier significantly reduced the NP size, whereas temperature had minimal influence on the particle size over the tested range. By varying the concentration of the stock solution, the size of the NPs can be adequately controlled. The minimum size of NPs prepared using a stock solution of 0.5 ml at 80°C into a 100 ml receiving solution was 70 nm with a narrow size distribution. Imaging by scanning electron microscopy revealed smooth spherical NPs and thermal and structural analysis showed only minor changes in properties in comparison with the source PHBV powder. Overall, the results show that glacial acetic acid is an appropriate alternative solvent for the dissolution of PHBV and the subsequent formation of biopolymer NPs.

KEYWORDS

biomaterials, biopolymers and renewable polymers, nanocrystals, nanoparticles, nanowires, synthesis and processing techniques

1 | INTRODUCTION

Polyhydroxyalkanoates (PHAs) are a class of biodegradable polyesters that are synthesized by several types of microbial monocultures and mixtures using a range of carbon-based feed stocks.[1–7] Selected bacteria synthesize and store PHAs in their cells under normal conditions or more commonly, under conditions of nutritional stress induced by a limitation of key nutrients (N, P, S, Mg, etc.) and an excess of carbon.[8] Several types of PHA polymers have been identified including poly-3-hydroxybutyrate (PHB)[9] and poly(3-hydroxybutyrate-co-3-hydroxyvalerate) (PHBV).[10] The different types of PHAs have been used in applications such as medicine[11–13] and packaging[10,14,15] among others.

Biopolymer micro and nanoparticles (NPs) are increasingly used in the field of drug delivery and therapeutics due to the biocompatibility and biodegradability of the

polymer coating.[16–18] Poly(lactic acid) is one such biopolymer that has been widely developed into NPs for the encapsulation of compounds including resveratrol,[19] aureusidin,[20] Withaferin-A,[21] guabiroba extract,[22] and curcumin.[23] Micro and NPs synthesized from PHA have also been developed and include PHBV microspheres containing superparamagnetic iron oxide for drug delivery and imaging,[12] NPs for cancer therapy,[24,25] and NPs for other drug delivery applications.[26–28]

There are several techniques employed to develop biopolymer NPs and these include nanoprecipitation[23,29] and more commonly, emulsion/solvent evaporation.[12,20,22,25] Regardless of the technique, the synthesis of micro and NPs generally involves the dissolution of the biopolymer in an organic solvent and PLA and PHAs are readily dissolved in acetone,[29] propylene carbonate,[30] chloroform,[23,31] and dichloromethane.[12,21,32–34] In recent years, there has been a shift towards using more environmentally friendly or "green" solvents in many industries[35] and this has also been the case for biopolymer extraction/processing[36,37] and chemical recycling.[38] Acetic acid is one such alternative solvent for PHAs and it has been reported that the properties of PHB films can be tailored using this solvent under varying temperatures.[39]

In this paper, we present a new technique to prepare PHBV nanoparticles using acetic acid as an alternative solvent via nanoprecipitation in water (solvent/non-solvent). The influence of temperature, solvent/stock solution volume, and the presence of emulsifiers were investigated as a function of the resulting NP size. Selected samples were further characterized by imaging, thermal and structural analysis to determine the suitability of using the acetic acid solvent system.

2 | EXPERIMENTAL

2.1 | Polymers and reagents

The PHBV polymer (ENMAT™ Thermoplastics Resin Y1000P, specific gravity 1.25, differential scanning calorimetry (DSC) melting temperature 170–176°C, 3% HV, M_w 240 kDa and M_w/M_n 2.6[40]), was provided in powder form by TianAn Biopolymer, China (courtesy of Professor Bronwyn Laycock, University of Queensland, Australia). Glacial acetic acid (purity 99.0–100.5%) was obtained from Ajax Finechem, Australia. Poly(vinyl alcohol) (PVA) (99 + % hydrolyzed; CAS 9002-89-5) and sodium hydroxide (>97%) were obtained from Sigma Aldrich (Sydney, Australia). Deionized water (DIW) was used in all experiments and was supplied using a Milli-Q system (Millipore, Billerica, MA, USA).

2.2 | Nanoparticle preparation and sizing

A stock solution of 0.5 wt% PHBV was prepared by dissolving PHBV powder in glacial acetic acid at 110°C. The prepared solution was filtered through a 0.45 μm Teflon filter to remove any undissolved polymer. The PHBV NPs were prepared by injecting the filtered stock solution into the receiving solution (100 ml DIW water containing NaOH equivalent to the molar amount of the acetic acid) under continuous stirring. The preparation conditions were optimized by varying the volume of stock solution (from 0.5 to 2 ml), the temperatures of the stock solution and receiving solution (from 70 to 100°C and 70 to 85°C, respectively), and the addition of 1 wt% of PVA emulsifier.

The particle size of NPs formed during each experiment was measured using a Malvern Zetasizer Nano ZS instrument (ATA Scientific, Taren Point, Australia). The temperature was maintained at 25°C and the diffractive index was set to 2.6 (provided by the PHBV supplier).

2.3 | Nanoparticle characterization

Suspensions containing PHBV NPs formed by the addition of 0.5, 1 and 2 ml of stock solution into 100 ml receiving solutions (with and without PVA) were filtered sequentially on a 0.45 μm PVDF filter to retain the particles smaller than 0.45 μm. The NPs collected on the cake layer of the filter were rinsed four times with DIW to remove the residual salt and were then dried on the filter at 45°C for 3 h. Due to the low concentration of NPs formed, this process was necessary to collect sufficient NPs for the subsequent characterization by scanning electron microscope (SEM), differential scanning calorimetry (DSC) and Fourier-transform infrared spectroscopy (FTIR) analyses.

The NPs were imaged using a SEM (Zeiss EVO LS15) using an electron high tension voltage of 3 kV and a working distance of 5.8–7.9 mm. The previously dried NPs were transferred onto a stud and subjected iridium coating for 30 s before observation.

DSC1 (Mettler Toledo, Greifensee, Switzerland) was used to evaluate the thermal properties of the prepared PHBV NPs and the powdered polymer. Samples weighing 10–12.5 mg were encapsulated in 30 μl aluminium crucibles. Samples were heated under nitrogen from 50 to 200°C at a heating rate of 10°C/min.

FTIR was used to assess any structural changes in PHBV during the dissolution and NP forming process. A Perkin Elmer Frontier™ FTIR spectrophotometer (Perkin Elmer, Waltham, MA, USA) fitted with a

diamond crystal attenuated total reflectance accessory was used to acquire the spectra of the PHBV powder and mixed NPs over the wavenumber range 4000–650 cm^{-1} using a resolution of 4 cm^{-1} and 64 scans per acquisition.

3 | RESULTS AND DISCUSSION

3.1 | Particle size analysis

3.1.1 | Influence of PVA addition on NP size

Water soluble polymers such as PVA are commonly used in the preparation of NPs as emulsifiers or stabilizers in order to facilitate control of the resulting NP size.[29,41–43] To investigate the influence of PVA on the PHBV NP size, a 1 wt% of PVA was prepared as the receiving solution to a 1 ml PHBV stock solution. Due to the large particle size obtained, the volume distributions rather than number distributions are presented as a function of particle size. The data for the 1 wt% PVA was further normalized by subtracting the volume of PVA from the total particle volume in the solution. This was necessary to remove the influence of the PVA from the resulting NP size analysis. As shown in Figure 1, the PHBV peak particle size was reduced by ca. 40% with the addition of 1 wt % PVA into the DIW receiving solution. This is due to the encapsulation capability of PVA which can inhibit the growth of small particles.[43] Other experiments using different concentrations of PVA and an alternative emulsifier (polyethylene glycol, PEG) were also performed and the results are shown in the Supporting Information (Table S1). In most cases, very large particles were formed (>1 μm) and when PEG was used, a visible precipitate formed so no further experiments using emulsifiers were conducted.

3.1.2 | Influence of stock solution volume on NP size

The particle size variation as a function of volume of the stock solution injected into the receiving solution is shown in Figure 2. The results show that as more stock solution is injected into the receiving solution, the formed PHBV NPs are larger and with a broader size distribution. This trend was also observed when using a lower receiving solution volume (50 ml) and up to 8 ml of stock solution (see Table S2). This phenomenon is attributed to the different nucleation kinetics[44] and although the critical nuclear size will be reduced as the saturation ratio increases (as defined by Dirksen and Ring[44]), the size change will be minimal in the case of saturation factors great than 4. Since the PHBV solubility was less than 5 mg/L in water (tested experimentally), the saturation ratio of all the injected solutions was greater than 5. With low injection volumes of the PHBV solution, primary homogeneous nucleation was the dominant process which results in the formation of small and uniform sized NPs.[45,46] As the injection volume of the stock solution was increased, primary heterogeneous and secondary nucleation became dominant leading to the

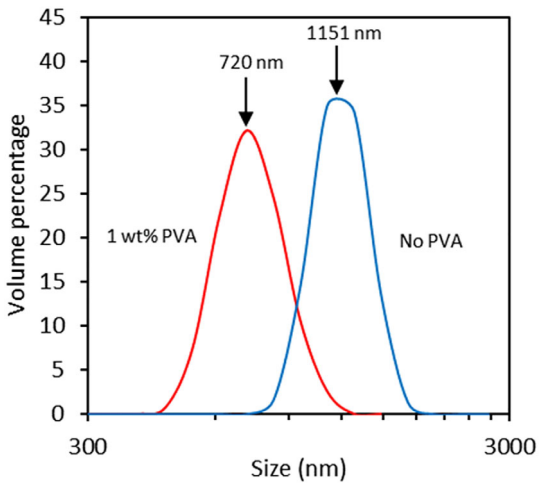

FIGURE 1 Size distribution of PHBV NPs with and without PVA in the receiving solution (1 ml stock solution at 70°C, 100 ml receiving solution at 25°C). NPs, nanoparticles; PHBV, poly (3-hydroxybutyrate-co-3-hydroxyvalerate); PVA, poly(vinyl alcohol) [Color figure can be viewed at wileyonlinelibrary.com]

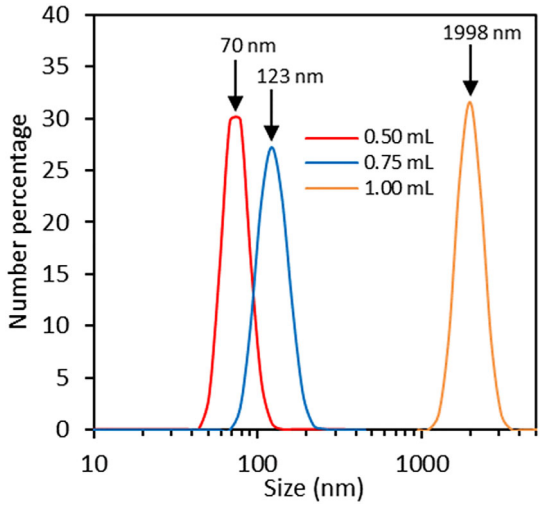

FIGURE 2 Size distribution of PHBV NPs with different volumes of stock solution (stock solution temperature 80°C in 100 ml receiving solution). NPs, nanoparticles; PHBV, poly (3-hydroxybutyrate-co-3-hydroxyvalerate) [Color figure can be viewed at wileyonlinelibrary.com]

formation of larger NPs with broader particle size distributions.[44]

3.1.3 | Influence of temperature on NP size

The temperatures of the stock solution and the receiving solution were varied in order to assess the influence of temperature on NP size. As shown in Figure 3a,b, neither the temperature of the stock solution or receiving solution resulted in significant variation in the NP size or resulting distribution. Over the temperature range tested, the PHBV is maintained in solute form in the acetic acid. The temperature of acetic acid solvent used to prepare PHB films is reported to impart the ability to control solvent evaporation and cooling as well as microscopic features.[39] In the present study, a lower receiving solution temperature could potentially offer significant energy savings by maintaining the receiving solution at room temperature. Other variables were also investigated including the concentration of the stock solution (Table S3), and the concentration of NaOH in the receiving solution (Table S4). In the examples shown in the Supporting Information, only minor variation in size is observed between the samples which is similar to the temperature variation shown in Figure 3.

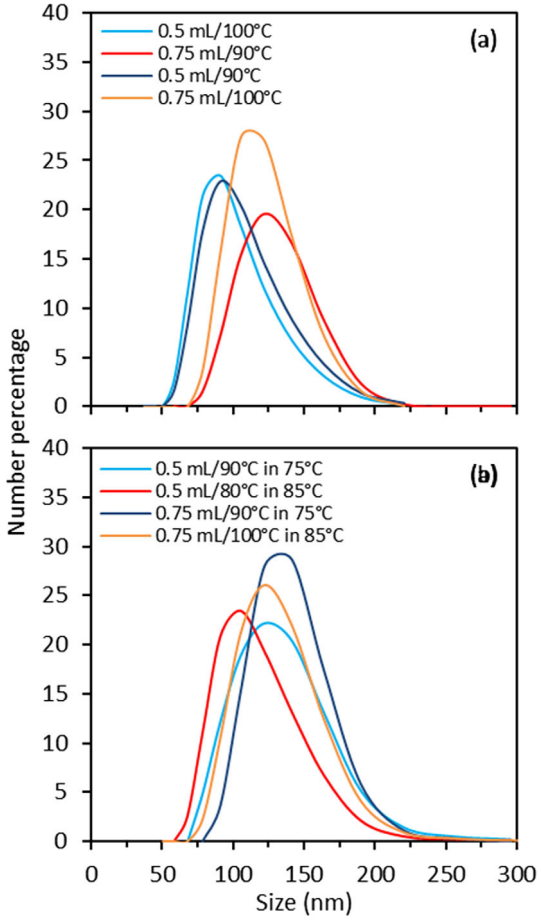

FIGURE 3 Size distribution of PHBV NPs obtained by varying (a) injected stock solution temperatures (receiving solution temperature 25°C) and (b) injected stock solution temperature in receiving solution temperature. A constant receiving solution volume of 100 ml was used. NPs, nanoparticles; PHBV, poly (3-hydroxybutyrate-co-3-hydroxyvalerate) [Color figure can be viewed at wileyonlinelibrary.com]

3.2 | Nanoparticle characterization

3.2.1 | SEM imaging of mixed NPs

Figure 4 shows the SEM images of NPs obtained from mixtures of the different stock solution additions. It is evident that there are few particles larger than 1 μm which is contrary to the Zetasizer results (see Figures 1 and 2). This difference may be due to agglomeration of the PHBV NPs[47] and/or size reduction of the NPs due to drying the samples for SEM imaging.[48] It is also evident that NPs that are smaller than 100 nm still are present although some surface particles were lost during the sample transfer to the sample stud. In general, the NPs appear smooth and round to oval in shape and not dissimilar to PHBV NPs prepared in chloroform.[48] Size analysis of 100 random particles was consistent with the observed Zetasizer results with approximate particle distributions of 42% 40–120 nm; 16% 120–160 nm; 12% 160–200 nm; 13% 200–300 nm; 10% 300–400 nm; and 7% 400+ nm. Further images of these NPs at different magnifications, and those formed in the presence of 1% PVA are shown in Figure S1. With regard to the sample prepared in the PVA emulsifier, it is evident that the PVA has coated the NPs resulting in much larger NPs that appear agglomerated. This was further confirmed by the subsequent FTIR and DSC data acquired which were dominated by PVA (data not shown).

3.2.2 | Thermal properties of NPs and PHBV powder

In Figure 5a, the DSC thermograms of the PHBV powder and NPs are shown based on the specific heat flow which was calculated by dividing the heat flow by the sample mass. The peak melting point (T_m) and the heat of fusion (ΔH_m) of the PHBV powder was 176.2°C and 98.15 J g^{-1} respectively, and the T_m and ΔH_m of the NPs was 162.5°C and 105.3 J g^{-1} respectively. The T_m value of the powder is within the range specified by the supplier (170–176°C) and similar T_m values for comparable grades of PHBV have been reported elsewhere ranging from

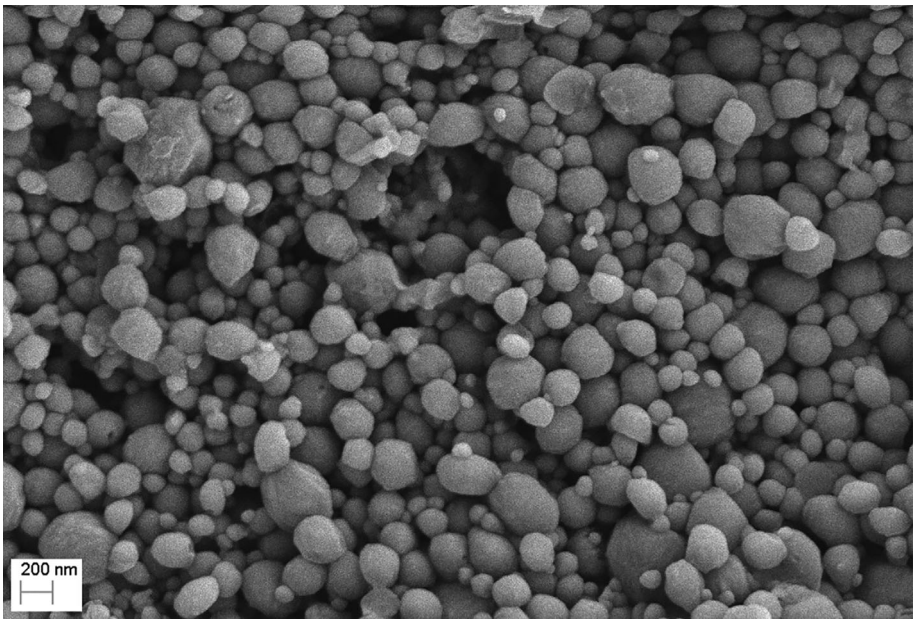

FIGURE 4 SEM images of mixed NPs at ×20,000 magnification (stock solution addition of 0.5, 1, and 2 ml in 100 ml receiving solution). NPs, nanoparticles; SEM, scanning electron microscope

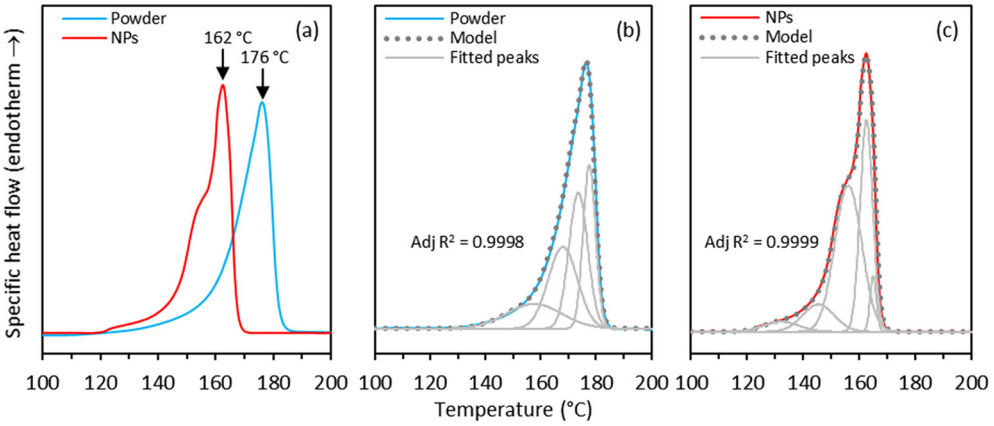

FIGURE 5 DSC thermograms of (a) PHBV powder and NPs (peak size ≈70 nm), (b) deconvoluted powder, and (c) deconvoluted NPs. DSC, differential scanning calorimetry; NPs, nanoparticles; PHBV, poly(3-hydroxybutyrate-co-3-hydroxyvalerate) [Color figure can be viewed at wileyonlinelibrary.com]

172 to 176°C.[49–53] The values of % crystallinity (χ_c) were calculated based on the ratio of the ΔH_m value of the samples and that of 100% crystalline PHBV (146 J g^{-1})[54] and were 67.2% and 72.1% for the PHBV powder and NPs respectively. The χ_c value of the powder is consistent with values reported elsewhere including 65%[55] and 66%[51] and it is widely reported that the χ_c and T_m vary with different HV content in PHBV samples.[50,51,56,57]

It is evident in Figure 5a that the specific heat flow of the PHBV NPs is greater than that of the PHBV powder. This phenomenon is due to an increased proportion of surface atoms as the size of particles decreases[58] and the very large surface area and surface energy of the NPs leading to the increase in ΔH_m and decrease in T_m[46,59] observed in comparison with the powder. Similar decreases in PHBV nanoparticle melting point have been reported which was attributed to a loss of degrees of freedom as a result of a decrease in crystallinity.[33] The increased ΔH_m of the PHBV NPs in the present study seems contrary to the general theory that the heat of fusion decreases with particle size due to the increase in the surface energy.[58,60] As shown in Figure 2, the distribution of the particle sizes is broad and the smaller particles would therefore melt earlier than the bigger ones. Figure 5a clearly shows shoulders on the thermograms in the case of the NPs with melting commencing at a lower temperature (ca. 120°C) and a prominent shoulder at ca. 150°C which suggests that smaller NPs are melting at different temperatures. The melted smaller particles will interconnect with the larger particles to increase the surface coverage and increase the thermal resistance to melting. To overcome this thermal resistance, more energy input is required and the resulting ΔH_m is greater than that of the PHBV powder. The melting of PHB films formed using acetic acid solvent at different temperatures showed two distinct melting peaks at all tested temperatures and a shoulder on the as-received PHB sample.[39] In this case, the lower melting peak was attributed to metastable crystals and the higher peak attributed to ordered crystals.[39] In the present study, the crystallization of the PHBV occurs more rapidly via spontaneous precipitation in water, thus more ordered crystals are formed that are unable to resolve into separate melting peaks at the tested DSC heating rate.

To further analyze the thermograms shown in Figure 5a, a Gaussian peak deconvolution procedure was applied to separate the component peaks of the PHBV powder (Figure 5b) and NPs (Figure 5c).[61,62] In the case of the powder, the thermogram was deconvoluted into four peaks whereas the thermogram of the NPs was deconvoluted into five peaks. In both cases, the adjusted R^2 value was >99.98% suggesting the peaks converged to an acceptable fit of the real data. The individual peaks and peak areas obtained from the deconvolution process are shown in Table 1. Both the powder and NPs are comprised of multiple crystal species that are overlapping although the presence of these peaks is more apparent in the case of the NPs. The largest contributing peak in the thermogram of the NPs occurs at 156°C which may suggest the formation of a considerable amount of metastable crystals than is immediately apparent from the untreated thermogram.[39]

3.2.3 | Structural properties of NPs and PHBV powder

Figure 6 shows the FTIR spectra of the powder and NPs and both spectra show similar features that are consistent with PHBV.[63–66] In Figure 6a, a small sharp peak is observed at 3447 cm^{-1} corresponding with the terminal OH groups of the PHBV[67] in both the powder and NPs. In addition to this peak, a slightly broader peak is observed in the region 3600–3200 cm^{-1} in the case of the NPs which may suggest some water entrapment on the surface. The peaks at 2998, 2977, 2934 and 2874 cm^{-1} are representative of —CH_3 ν(as), —CH_3 ν(s), —CH_2 ν(as) and —CH_3 ν(s) groups, respectively.[68,69] There are no significant differences between the spectra of the NPs or the powder in this region suggesting no major changes in the PHBV structure following the formation of the NPs. In particular, no changes are observed in the peak at 2934 cm^{-1} (—C═H) which would otherwise indicate bond breakage.[70]

Figure 6b shows the characteristic carbonyl peak of PHBV at ca. 1720 cm^{-1} (crystalline state) with a small shoulder at ca. 1741 cm^{-1} (amorphous state).[48,64,65,71] A small peak is observed at 1687 cm^{-1} which may result from the interaction between terminal OH groups and C═O groups.[72,73] There is some subtle shifting in the main carbonyl peak which may suggest some changes in the crystallinity which was observed in the DSC data. The carbonyl peaks in Figure 6b were further examined by applying a Gaussian deconvolution process[64,74] and Figure 7 shows the resulting spectra. In both cases, the main peaks were deconvoluted into five separate peaks and the adjusted R^2 values were >99.99% suggesting acceptable fits to the real data. The peaks and peak areas obtained from the deconvolution process are shown in Table 2 and similar deconvolutions of the carbonyl peaks have been reported and the individual peaks assigned to the C═O bands in the crystalline and amorphous regions.[72,73,75] In the present study, the amorphous C═O peaks at 1743 and 1745 cm^{-1} contribute 12% and 11% of the area of the combined peaks of the powder and NPs respectively. A similar amorphous peak ratio for PHBV powder of 9.6% has been reported and in the same study, a ratio of 18.6% was determined for PHBV nanofibers

TABLE 1 Data obtained from deconvoluted thermograms

	Powder		NPs	
	T_m (°C)	Area (%)	T_m (°C)	Area (%)
Peak 1	157.6	16.5%	132.1	4.3%
Peak 2	168.0	28.6%	145.3	10.6%
Peak 3	173.6	30.5%	156.0	48.1%
Peak 4	177.6	24.4%	162.5	32.6%
Peak 5	-	-	164.9	4.4%

Abbreviation: NPs, nanoparticles.

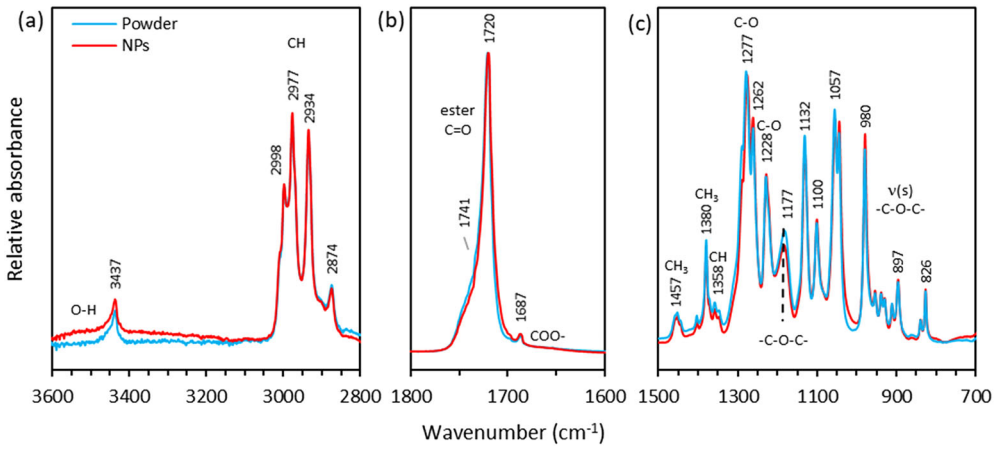

FIGURE 6 FTIR spectra of PHBV powder and NPs (peak size ≈70 nm) in the wavenumber regions (a) 3600–2800 cm^{-1}, (b) 1800–1600 cm^{-1}, and 1500–700 cm^{-1}. FTIR, Fourier-transform infrared spectroscopy; PHBV, poly (3-hydroxybutyrate-co-3-hydroxyvalerate); NPs, nanoparticles [Color figure can be viewed at wileyonlinelibrary.com]

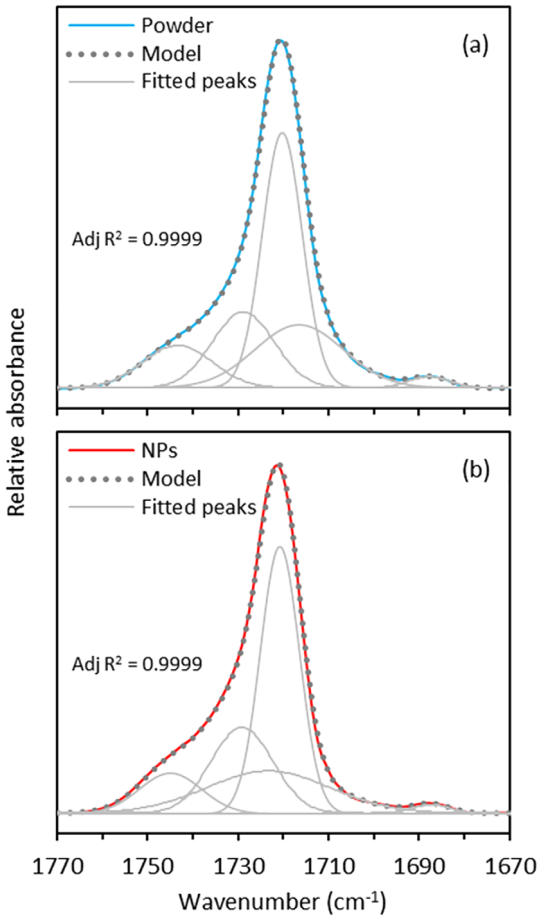

FIGURE 7 Deconvoluted FTIR spectra of (a) powder and (b) NPs (peak size ≈70 nm) in the wavenumber region 1770–1670 cm^{-1}. FTIR, Fourier-transform infrared spectroscopy; NPs, nanoparticles [Color figure can be viewed at wileyonlinelibrary.com]

TABLE 2 Data obtained from deconvoluted FTIR peaks

	Powder		NPs	
	Peak (cm^{-1})	Area (%)	Peak (cm^{-1})	Area (%)
Peak 1	1743	12	1745	11
Peak 2	1729	20	1729	22
Peak 3	1720	43	1723	22
Peak 4	1716	23	1721	44
Peak 5	1688	2	1687	1

Abbreviation: FTIR, Fourier-transform infrared spectroscopy.

(18.6%).[73] In this case, the formation of the nanofibers via electrospinning was suggested to impede the crystallization of the PHBV.

In Figure 6c, further peaks characteristic of PHBV are observed including: 1457 and 1380 cm^{-1} (CH_3), 1358 cm^{-1} (CH), 1277–1100 cm^{-1} (C—O, C—O—C), and 1057–826 cm^{-1} (C—O, C—C).[30,63,65,68,70,76–78] Similar to the other spectral regions, the peaks of the PHBV powder and NPs in this region are similar with no significant differences suggesting the overall PHBV chemical structure is unaffected by the formation of the NPs. The peaks at 1380 and 1180 cm^{-1} are insensitive and sensitive to crystallinity respectively, and their ratio has been used to define a crystallinity index (CI).[79,80] Based on this ratio, the CI values of the PHBV powder and NPs were 0.91 and 0.98, respectively. Reported CI values of PHBV include 0.96[65] and decrease from 0.99 to 0.81 with increasing HV content.[79] The higher crystallinity index in the case of the NPs in the present study is consistent with the higher crystallinity measured using DSC. Overall, the FTIR results show no significant differences in the structural characteristics as a result of the dissolution of the PHBV powder in acetic acid to form the NPs.

4 | CONCLUSIONS

In order to eliminate the use of toxic organic solvents, NPs were formed by dissolving PHBV powder in glacial acetic acid followed by precipitation in water. The NP size was reduced by 40% when the receiving solution contained PVA as an emulsifier. Further reductions in NP size were achieved by reducing the total volume of the stock PHBV solution injected into the receiving solution with a minimum NP size of 70 nm obtained. Varying the injected stock solution temperatures and receiving solution temperatures at a constant receiving solution volume had minimal influence on the size with NPs between 100–150 nm obtained although the size distributions were relatively broad. The SEM imaging of mixed NPs revealed smooth, round particles with a range of sizes up to 1 μm in diameter with some sub-100 nm NPs present. Thermal analysis of the same mixed NPs using DSC showed that the T_m of the NPs was 14°C lower than that of the powder, although the χ_c was higher and the thermogram of the NPs contained multiple shoulders. Deconvolution of the thermograms revealed both the NPs and powder were comprised of multiple peaks that suggest the presence of different crystal types with an additional peak contributing to the converged NP thermogram. The FTIR analysis showed only minor changes in some characteristic peaks between the spectra of the NPs and powder and deconvolution of the main carbonyl peaks suggested minimal changes in crystallinity. Overall, the use of glacial acetic acid was shown to be a suitable substitute for organic solvents in the dissolution of PHBV to form NPs of various sizes.

ACKNOWLEDGMENT

Open access publishing facilitated by Victoria University, as part of the Wiley - Victoria University agreement via the Council of Australian University Librarians.

AUTHOR CONTRIBUTIONS

Jianhua Zhang: Conceptualization (equal); data curation (equal); formal analysis (equal); investigation (lead); methodology (lead); visualization (supporting); writing – original draft (equal); writing – review and editing (equal). **Marlene J. Cran:** Conceptualization (equal); data curation (equal); formal analysis (equal); investigation (supporting); methodology (supporting); visualization (lead); writing – original draft (equal); writing – review and editing (equal).

DATA AVAILABILITY STATEMENT

Research data are not shared.

ORCID

Jianhua Zhang https://orcid.org/0000-0002-8674-0485
Marlene J. Cran https://orcid.org/0000-0002-6000-8093

REFERENCES

[1] V. Gowda, S. Shivakumar, *Braz. Arch. Biol. Technol.* **2014**, *57*, 55.
[2] S. Obruca, P. Benesova, S. Petrik, J. Oborna, R. Prikryl, I. Marova, *Process Biochem.* **2014**, *49*, 1409.
[3] C.-S. Wu, *J. Polym. Environ.* **2014**, *22*, 384.
[4] M. V. Arcos-Hernández, B. Laycock, B. C. Donose, S. Pratt, P. Halley, S. Al-Luaibi, A. Werker, P. A. Lant, *Eur. Polym. J.* **2013**, *49*, 904.
[5] C. M. Chan, P. Johansson, P. Magnusson, L.-J. Vandi, M. Arcos-Hernandez, P. Halley, B. Laycock, S. Pratt, A. Werker, *Polym. Degrad. Stab.* **2017**, *144*, 110.
[6] M. V. Arcos-Hernandez, S. Pratt, B. Laycock, P. Johansson, A. Werker, P. A. Lant, *Waste Biomass Valoriz.* **2012**, *4*, 117.
[7] P. Luangthongkam, B. Laycock, P. Evans, P. Lant, S. Pratt, *New Biotechnol.* **2019**, *53*, 49.
[8] S. Khanna, A. K. Srivastava, *Process Biochem.* **2005**, *40*, 607.
[9] N. Batool, N. Ilyas, *Int J Biosci* **2014**, *5*, 298.
[10] E. Bugnicourt, P. Cinelli, A. Lazzeri, V. Alvarez, *Express Polym Lett* **2014**, *8*, 791.
[11] W. H. Chen, B. L. Tang, Y. W. Tong, *in 13th International Conference on Biomedical Engineering. IFMBE Proceedings* (Eds: C. T. Lim, J. C. H. Goh), Vol 23. Springer, Berlin, Heidelberg **2009**. https://doi.org/10.1007/978-3-540-92841-6_296
[12] W. Li, J. Zaloga, Y. Ding, Y. Liu, C. Janko, M. Pischetsrieder, C. Alexiou, A. R. Boccaccini, *Sci. Rep.* **2016**, *6*, 23140.
[13] M. Koller, P. Hesse, R. Bona, C. Kutschera, A. Atlic, G. Braunegg, *Macromol. Symp.* **2007**, *253*, 33.
[14] M. J. Fabra, A. López-Rubio, J. M. Lagaron, in *Smart Polymers and their Applications* (Eds: M. R. Aguilarand, J. S. Román), Woodhead Publishing, Cambridge **2014**, p. 476.
[15] D. Plackett, I. Siró, in *Multifunctional and Nanoreinforced Polymers for Food Packaging* (Ed: J.-M. Lagarón), Woodhead Publishing, Cambridge **2011**, p. 498.
[16] J. M. Anderson, M. S. Shive, *Adv. Drug Deliv. Rev.* **2012**, *64*, 72.
[17] H. N. Nguyen, P. T. Ha, A. S. Nguyen, D. T. Nguyen, H. D. Do, Q. N. Thi, M. N. H. Thi, *Adv. Nat. Sci. Nanosci. Nanotechnol.* **2016**, *7*, 025001.
[18] F. Rancan, D. Papakostas, S. Hadam, S. Hackbarth, T. Delair, C. Primard, B. Verrier, W. Sterry, U. Blume-Peytavi, A. Vogt, *Pharm. Res.* **2009**, *26*, 2027.
[19] G. Lindner, N. M. Khalil, R. M. Mainardes, *Sci. World J.* **2013**, *2013*, 506081.
[20] M. Roussaki, A. Gaitanarou, P. C. Diamanti, S. Vouyiouka, C. Papaspyrides, P. Kefalas, A. Detsi, *Polym. Degrad. Stab.* **2014**, *108*, 182.
[21] Z. A. Khan, A. K. A. Mandal, R. Abinaya, K. Krithika, *Middle-East J. Sci. Res.* **2013**, *14*, 544.
[22] M. C. Pereira, L. E. Hill, R. C. Zambiazi, S. Mertens-Talcott, S. Talcott, C. L. Gomes, *LWT Food Sci. Technol.* **2015**, *63*, 100.
[23] M. H. M. Leung, T. Harada, S. Dai, T. W. Kee, *Langmuir* **2015**, *31*, 11419.
[24] P. Solar, N. Herrera, D. Cea, S. Devis, F. Gonzalez-Nilo, N. Juica, M. Moreno, M. N. Gai, I. Brescia, S. Henríquez, L. Velasquez, *J. Clust. Sci.* **2021**, *32*, 1563. https://doi.org/10.1007/s10876-020-01912-6.
[25] F. Masood, P. Chen, T. Yasin, N. Fatima, F. Hasan, A. Hameed, *Mater. Sci. Eng. C* **2013**, *33*, 1054.
[26] A. Shrivastav, H.-Y. Kim, Y.-R. Kim, *Biomed. Res. Int.* **2013**, *2013*, 581684.
[27] C. V. Nachiyar, A. B. Devi, S. K. R. Namasivayam, A. M. Rabel, *Res J Pharm Biol Chem Sci* **2015**, *6*, 116.
[28] C. Vilos, F. A. Morales, P. A. Solar, N. S. Herrera, F. D. Gonzalez-Nilo, D. A. Aguayo, H. L. Mendoza, J. Comer, M. L. Bravo, P. A. Gonzalez, S. Kato, M. A. Cuello, C. Alonso, E. J. Bravo, E. I. Bustamante, G. I. Owen, L. A. Velasquez, *Biomaterials* **2013**, *34*, 4098.
[29] M. Wrona, M. J. Cran, C. Nerín, S. W. Bigger, *Carbohydr. Polym.* **2017**, *156*, 108.
[30] V. K. Rastogi, P. Samyn, *Express Polym Lett* **2020**, *14*, 115.
[31] F. V. Leimann, L. Cardozo Filho, C. Sayer, P. Araújo, *Braz J Chem Eng* **2013**, *30*, 369.
[32] E. B. Freiberger, K. C. Kaufmann, E. Bona, P. H. Hermes de Araújo, C. Sayer, F. V. Leimann, O. H. Gonçalves, *LWT Food Sci. Technol.* **2015**, *64*, 381.
[33] P. Solar, G. Gonzalez, C. Vilos, N. Herrera, N. Juica, M. Moreno, F. Simon, L. Velasquez, *J Nanobiotechnol* **2015**, *13*, 14.
[34] R. Vijayamma, H. J. Maria, S. Thomas, E. I. Shishatskaya, E. G. Kiselev, I. V. Nemtsev, A. A. Sukhanova, T. G. Volova, *J Appl Pol. Sci.* **2021**, *139*, 51756.
[35] W. Xie, T. Li, A. Tiraferri, E. Drioli, A. Figoli, J. C. Crittenden, B. Liu, *ACS Sustain. Chem. Eng.* **2021**, *9*, 50.
[36] N. S. Kurian, B. Das, *Int. J. Biol. Macromol.* **2021**, *183*, 1881.
[37] H. Mahmood, M. Moniruzzaman, *Biotechnol. J.* **2019**, *14*, 1900072.
[38] X. Yang, K. Odelius, M. Hakkarainen, *ACS Sustain. Chem. Eng.* **2014**, *2*, 2198.
[39] P. Anbukarasu, D. Sauvageau, A. Elias, *Sci. Rep.* **2015**, *5*, 17884.
[40] V. Jost, R. Kopitzky, *Chem. Biochem. Eng. Q.* **2015**, *29*, 221.
[41] R. Kumar, P. F. Siril, *Materials Today: Proceedings* **2016**, *3*, 2261.
[42] A. M. Deliormanli, A. C. Yenice, *Express Polym Lett* **2021**, *15*, 641.

[43] P. S. Roy, J. Bagchi, S. K. Bhattacharya, *Transit. Met. Chem.* **2009**, *34*, 447.
[44] J. A. Dirksen, T. A. Ring, *Chem. Eng. Sci.* **1991**, *46*, 2389.
[45] D. Zhu, X. Jiang, C. Zhao, X. Sun, J. Zhang, J.-J. Zhu, *Chem. Commun.* **2010**, *46*, 5226.
[46] L. Gunawan, G. Johari, *J. Phys. Chem. C* **2008**, *112*, 20159.
[47] I. Gosens, J. A. Post, L. J. de la Fonteyne, E. H. Jansen, J. W. Geus, F. R. Cassee, W. H. de Jong, *Part. Fibre Toxicol.* **2010**, *7*, 37.
[48] M. Otroj, S. Taymouri, J. Varshosaz, M. Mirian, *J Drug Del Sci. Technol.* **2020**, *56*, 101570.
[49] Z. Li, C. Reimer, T. Wang, A. K. Mohanty, M. Misra, *Polymer* **2020**, *12*, 1300.
[50] L. Shang, Q. Fei, Y. H. Zhang, X. Z. Wang, D.-D. Fan, H. N. Chang, *J. Polym. Environ.* **2011**, *20*, 23.
[51] J. Bossu, H. Angellier-Coussy, C. Totee, M. Matos, M. Reis, V. Guillard, *Biomacromolecules* **2020**, *21*, 4709.
[52] A. P. B. Silva, L. S. Montagna, F. R. Passador, M. C. Rezende, A. P. Lemes, *Express Polym Lett* **2021**, *15*, 987.
[53] M. Cunha, B. Fernandes, J. A. Covas, A. A. Vicente, L. Hilliou, *J. Appl. Polym. Sci.* **2016**, *133*, 42165.
[54] P. J. Barham, A. Keller, E. L. Otun, P. A. Holmes, *J. Mater. Sci.* **1984**, *19*, 2781.
[55] M. C. Righetti, P. Cinelli, N. Mallegni, A. Stäbler, A. Lazzeri, *Polymer* **2019**, *11*, 308.
[56] V. Jost, *Express Polym Lett* **2018**, *12*, 429.
[57] Y. Wang, R. Chen, J. Cai, Z. Liu, Y. Zheng, H. Wang, Q. Li, N. He, *PLoS One* **2013**, *8*, e60318.
[58] J. Sun, S. L. Simon, *Thermochim. Acta* **2007**, *463*, 32.
[59] W. H. Qi, *Physica B Cond Matter* **2005**, *368*, 46.
[60] R. Defay, I. Prigogine, A. Bellemans, *Surface Tension and Adsorption*, Wiley, New York **1966**.
[61] A. Michael, Y. N. Zhou, M. Yavuz, M. I. Khan, *Thermochim. Acta* **2018**, *665*, 53.
[62] B. Szepcsik, B. Pukánszky, *J. Therm. Anal. Calorim.* **2018**, *133*, 1371.
[63] M. P. Arrieta, J. López, D. López, J. M. Kenny, L. Peponi, *Eur. Polym. J.* **2015**, *73*, 433.
[64] L. Wei, N. M. Stark, A. G. McDonald, *Green Chem.* **2015**, *17*, 4800.
[65] J. Li, M. F. Lai, J. J. Liu, *J. Appl. Polym. Sci.* **2004**, *92*, 2514.
[66] B. Laycock, P. Halley, S. Pratt, A. Werker, P. Lant, *Prog. Polym. Sci.* **2014**, *39*, 397.
[67] M. Sharma, H. K. Dhingra, *Int J Sci Res* **2015**, *4*, 1895.
[68] Y.-X. Weng, X.-L. Wang, Y.-Z. Wang, *Polym. Test.* **2011**, *30*, 372.
[69] D. M. Panaitescu, E. R. Ionita, C.-A. Nicolae, A. R. Gabor, M. D. Ionita, R. Trusca, B.-E. Lixandru, I. Codita, G. Dinescu, *Polymers* **2018**, *10*, 1249.
[70] P. Phukon, J. P. Saikia, B. K. Konwar, *Colloids Surf. B. Biointerfaces* **2012**, *92*, 30.
[71] O. Raşoga, L. Sima, M. Chiriţoiu, G. Popescu-Pelin, O. Fufă, V. Grumezescu, M. Socol, A. Stănculescu, I. Zgură, G. Socol, *Appl. Surf. Sci.* **2017**, *417*, 204.
[72] J. Zhang, H. Sato, I. Noda, Y. Ozaki, *Macromolecules* **2005**, *38*, 4274.
[73] A. C. Mottin, E. Ayresa, R. L. Oréficec, J. J. D. Câmaraa, *Mater. Res.* **2016**, *19*, 57.
[74] F. Li, H.-Y. Yu, Y.-Y. Wang, Y. Zhou, H. Zhang, J.-M. Yao, S. Y. H. Abdalkarim, K. C. Tam, *J. Agric. Food Chem.* **2019**, *67*, 10954.
[75] C. Wang, C.-H. Hsu, I. H. Hwang, *Polymer* **2008**, *49*, 4188.
[76] P. Tomietto, P. Loulergue, L. Paugam, J.-L. Audic, *Sep Purif Technol* **2020**, *252*, 117419.
[77] A. M. Diez-Pascual, A. L. Diez-Vicente, *Int. J. Mol. Sci.* **2014**, *15*, 10950.
[78] M. Umesh, K. Priyanka, B. Thazeem, K. Preethi, *Arab. J. Sci. Eng.* **2017**, *42*, 2361.
[79] S. Bloembergen, D. A. Holden, G. K. Hamer, T. L. Bluhm, R. H. Marchessault, *Macromolecules* **1986**, *19*, 2865.
[80] V. Sridhar, I. Lee, H. H. Chun, H. Park, *Express Polym Lett* **2013**, *7*, 320.

SUPPORTING INFORMATION

Additional supporting information may be found in the online version of the article at the publisher's website.

How to cite this article: J. Zhang, M. J. Cran, *J. Appl. Polym. Sci.* **2022**, *139*(23), e52319. https://doi.org/10.1002/app.52319